NANO LETTERS

2008
Vol. 8, No. 9
2906-2912

Microfluidic Platform for Controlled Synthesis of Polymeric Nanoparticles

Rohit Karnik,[†,‡] Frank Gu,[†,§] Pamela Basto,[§,||] Christopher Cannizzaro,[§] Lindsey Dean,[§] William Kyei-Manu,[§] Robert Langer,[§,||,⊥] and Omid C. Farokhzad*[,⊥,#]

Department of Mechanical Engineering, Massachusetts Institute of Technology, Cambridge, Massachusetts 02139, Department of Chemical Engineering, Massachusetts Institute of Technology, Cambridge, Massachusetts 02139, Harvard−MIT Division of Health Sciences and Technology, Massachusetts Institute of Technology, Cambridge, Massachusetts 02139, MIT−Harvard Center for Cancer Nanotechnology Excellence, Massachusetts Institute of Technology, Cambridge, Massachusetts 02139, and Laboratory of Nanomedicine and Biomaterials and Department of Anesthesiology, Brigham and Women's Hospital, Harvard Medical School, Boston, Massachusetts 02115

Received June 17, 2008

ABSTRACT

A central challenge in the development of drug-encapsulated polymeric nanoparticles is the inability to control the mixing processes required for their synthesis resulting in variable nanoparticle physicochemical properties. Nanoparticles may be developed by mixing and nanoprecipitation of polymers and drugs dissolved in organic solvents with nonsolvents. We used rapid and tunable mixing through hydrodynamic flow focusing in microfluidic channels to control nanoprecipitation of poly(lactic-*co*-glycolic acid)-*b*-poly(ethylene glycol) diblock copolymers as a model polymeric biomaterial for drug delivery. We demonstrate that by varying (1) flow rates, (2) polymer composition, and (3) polymer concentration we can optimize the size, improve polydispersity, and control drug loading and release of the resulting nanoparticles. This work suggests that microfluidics may find applications for the development and optimization of polymeric nanoparticles in the newly emerging field of nanomedicine.

The ability of microfluidics to rapidly mix reagents, provide homogeneous reaction environments, continuously vary reaction conditions, and add reagents at precise time intervals during reaction progression has made it an attractive technology for a myriad of applications.[1,2] Over the past decade, microfluidic devices have enabled screening of a variety of reaction conditions by systematically varying flow rates, temperature, and reactant concentrations in order to optimize the quality of the resulting products using very small amounts of reagents.[2,3] In parallel, there has been an increasing interest in the development of novel nanoparticle and microparticle technologies for drug delivery, imaging, bioanalysis, photonics, and optoelectronic applications. The convergence of microfluidic and particle technologies has shown considerable promise allowing for the development of inorganic nanoparticles[4–9] and microparticles[10] and, in some cases with narrow size distribution or distinct shapes, addressing an important challenge for their maximal exploitation. Relatively little has been done to harness the benefits of microfluidics for the synthesis of organic nanoparticles. This is particularly important since the synthesis of biodegradable polymeric nanoparticles by bulk mixing and nanoprecipitation[11] of drugs and biodegradable polymeric precursors typically lacks control over the mixing processes, which may compromise the properties of the resulting nanoparticles. Rapid and tunable mixing in microfluidics may allow for better control over the process of nanoprecipitation and also enable screening of various formulation conditions on a single platform by varying parameters such as flow rates, precursor composition, and mixing time.

Our groups and others have previously used poly(lactide-*co*-glycolide)-*b*-poly(ethylene glycol) (PLGA-PEG) block

* To whom correspondence should be addressed: Laboratory of Nanomedicine and Biomaterials and Department of Anesthesiology, Brigham and Women's Hospital, Harvard Medical School, Boston, MA 02115; e-mail, ofarokhzad@zeus.bwh.harvard.edu.

† These authors contributed equally to this paper.

‡ Department of Mechanical Engineering, Massachusetts Institute of Technology.

§ Department of Chemical Engineering, Massachusetts Institute of Technology.

|| Harvard−MIT Division of Health Sciences and Technology, Massachusetts Institute of Technology.

⊥ MIT−Harvard Center for Cancer Nanotechnology Excellence, Massachusetts Institute of Technology.

Laboratory of Nanomedicine and Biomaterials and Department of Anesthesiology, Brigham and Women's Hospital, Harvard Medical School.

10.1021/nl801736q CCC: $40.75
Published on Web 07/26/2008

copolymers as a model biodegradable and biocompatible biomaterial to synthesize nanoparticles by nanoprecipitation for a variety of biomedical applications.[12–16] The PLGA component of the PLGA-PEG nanoparticles provides a biodegradable and biocompatible matrix for encapsulation and controlled release of drugs, while the PEG component provides "stealth" properties for immune evasion and long circulation half-life in blood. Nanoprecipitation offers the advantages of simple and gentle formulation under ambient conditions without the use of chemical additives or harsh formulation processes. However, typical synthesis of PLGA-PEG nanoparticles by nanoprecipitation involves dropwise addition of polymer−organic solvent solution into a larger quantity of water, resulting in slow and uncontrolled mixing. Nanoprecipitation through rapid and controlled mixing may enable the formation of more homogeneous PLGA-PEG nanoparticles and provide better control of nanoparticle properties such as size, surface characteristics, and drug loading. Here we demonstrate that rapid and tunable microfluidic mixing can be used to synthesize drug-encapsulated biodegradable polymeric PLGA-PEG nanoparticles with defined size, lower polydispersity, and higher drug loading with slower release.

Microfluidics has previously been used by several researchers for synthesis of polymeric particles through the formation of emulsions.[12,17–21] The emulsion method relies on hydrodynamic instability to break up an immiscible polymeric solution into droplets,[22] which subsequently form microscale particles through cross-linking or solvent evaporation. The method presented in this paper is distinct as it involves formation of nanoparticles through self-assembly of block copolymers using flow focusing to rapidly mix miscible polymer solutions with water. Emulsion−solvent evaporation[24] is another well-known bulk method for formation of nanoparticles. The size of nanoparticles made by this method is also generally large (>150 nm) around 200 nm. It is well-known that polymeric nanoparticles with such large size can be easily scavenged by organs of the reticuloendothelial system, resulting in short circulation half-life and high systemic toxicity.[23] Although small PLGA-based nanoparticles with diameters <100 nm can be easily obtained via nanoprecipitation, these nanoparticles have poor drug encapsulation and rapid drug release, compounded with high polydispersity. In this study, we aimed to understand the self-assembly of PLGA-PEG during nanoprecipitation, while optimizing the physiochemical properties of these nanoparticles.

Synthesis of PLGA-PEG Nanoparticles by Hydrodynamic Flow Focusing. We synthesized PLGA-PEG nanoparticles in a microfluidic channel by rapidly mixing polymer−acetonitrile solutions and water using hydrodynamic flow focusing[25] in a controlled nanoprecipitation process. In hydrodynamic flow focusing, the fluid stream to be mixed flows along the central channel meeting two adjacent streams flowing at higher flow rates (Figure 1b). At low Reynolds numbers, the central stream is squeezed into a narrow stream between the two adjacent streams. The narrow width of the focused stream then enables rapid mixing

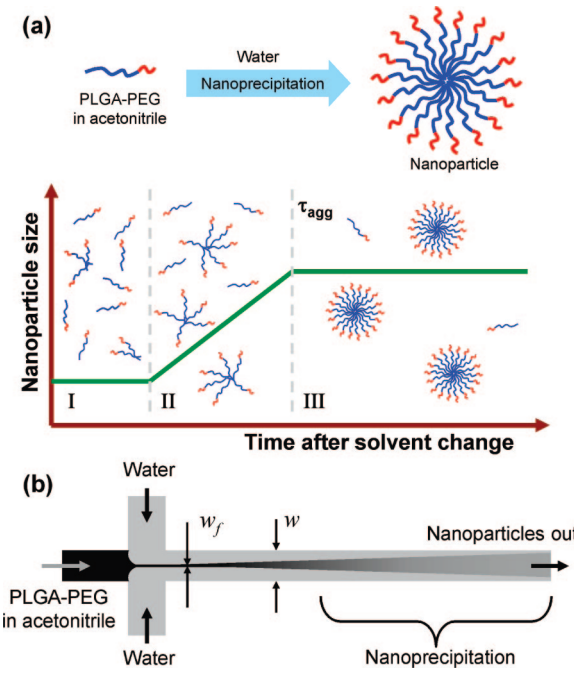

Figure 1. Nanoprecipitation of PLGA-PEG copolymers. (a) PLGA-PEG diblock copolymers self-assemble into nanoparticles when a water-miscible solution of the polymers is mixed with water, in which the PLGA block is poorly soluble. The process occurs in three stages involving nucleation of nanoparticles, growth through aggregation, and results in kinetically locked nanoparticles after a characteristic aggregation time scale τ_{agg}. (b) The process of mixing can be carried out in a microfluidic device using hydrodynamic flow focusing, where the polymer stream is focused into a thin stream between two water streams with higher flow rates. Rapid mixing and nanoprecipitation occur due to diffusion of the solvent out of the focused stream and diffusion of water into the focused stream.

through diffusion. We can estimate the mixing time (τ_{mix}) for hydrodynamic flow focusing using a two-dimensional model as (see Supporting Information)

$$\tau_{mix} \sim \frac{w_f^2}{4D} \approx \frac{w^2}{9D}\frac{1}{(1+1/R)^2} \quad (1)$$

where D is diffusivity of the solvent, w_f is width of the focused stream, w is channel width, and R is the ratio of flow rate of the polymeric stream to the total flow rate of water.

Microfluidic devices were fabricated with poly(dimethylsiloxane) (PDMS) using a standard micromolding process (see Supporting Information). The microchannel for hydrodynamic flow focusing was 20 μm wide, 60 μm high, and 1 cm long. Flow rates were controlled using syringe pumps. For $D = 10^{-9}$ m^2/s and $w = 20$ μm, eq 1 predicts a mixing time in the range of 0.04−0.4 ms for typical flow ratios ($R = 0.03-0.1$) in our device. Hydrodynamic flow focusing was easily achieved in the device with the polymer−organic solvent solution in the central focused stream and water in the adjacent streams (Figure 2a). To confirm formation of nanoparticles in our device, the outlet stream resulting from mixing of 50 mg/mL $PLGA_{15K}$-$PEG_{3.4K}$ solution in acetonitrile at total flow rates of 0.5 and 10 μL/min for the acetonitrile and water streams, respectively, was dispersed

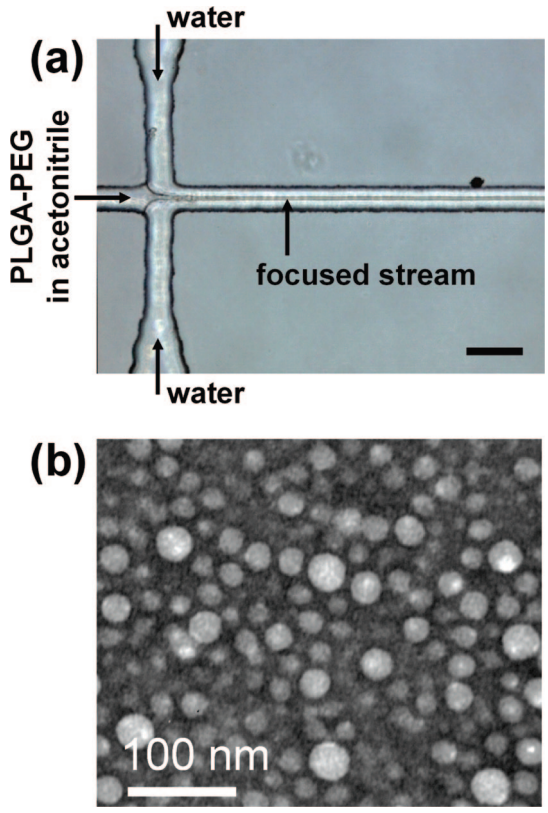

Figure 2. Nanoprecipitation by hydrodynamic flow focusing. (a) A microfluidic device for hydrodynamic flow focusing of polymeric nanoparticles in water. Scale bar 50 μm. (b) TEM image of nanoparticles synthesized by nanoprecipitation of $PLGA_{15K}$-$PEG_{3.4K}$ by hydrodynamic flow focusing showing spherical PLGA core−PEG corona structure of the nanoparticles.

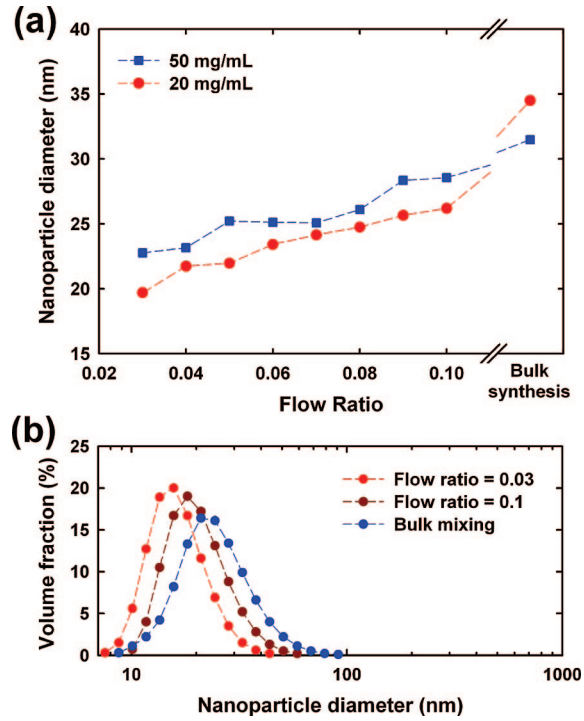

Figure 3. Effect of flow ratio on nanoparticle size. (a) Size of nanoparticles obtained by nanoprecipitation using hydrodynamic flow focusing of $PLGA_{15K}$-$PEG_{3.4K}$ decreased as the flow ratio was decreased and rate of mixing was increased. Nanoparticles thus obtained were smaller in size than those obtained by bulk synthesis. (b) The homogeneity of nanoparticles obtained by nanoprecipitation of 20 mg/mL $PLGA_{15K}$-$PEG_{3.4K}$ increased as the rate of mixing increased, corresponding to smaller flow ratios. Size measurements were obtained using dynamic light scattering.

and imaged using a transmission electron microscope (see Supporting Information). Spherical nanoparticles with diameters typically in the range of 10−50 nm were observed (Figure 2b). The hydrophobic PLGA core was stained with magnesium uranyl acetate, while the hydrophilic PEG corona did not get stained and appeared as a dark halo surrounding the PLGA core. Size measurements using dynamic light scattering yielded a *Z*-average diameter of about 24 nm which was consistent with the transmission electron microscopy (TEM) image. For comparison with conventional synthesis by slow mixing, 3 μL of the same polymeric solution was pipetted into 60 μL of water, yielding larger nanoparticles with a *Z*-average diameter of 31 nm. For the same batch of PLGA-PEG polymer, *Z*-average nanoparticle size was typically reproducible to within ±1 nm between different experiments, demonstrating the robustness of on-chip synthesis; however, this degree of reproducibility was not possible between different batches of polymers. We also did not observe significant precipitates in the microchannel, which may be expected as the PLGA-PEG polymer is transferred to a poor solvent (water) in the device. This result establishes hydrodynamic flow focusing as a simple, robust, and reproducible technology for nanoprecipitation of PLGA-PEG nanoparticles.

We further varied the mixing time for solvent exchange by changing the flow ratio of water and acetonitrile streams from 10 μL/min:1 μL/min to 10 μL/min:0.3 μL/min, resulting in mixing time τ_{mix} ranging from approximately 0.4 to 0.04 ms (eq 1). We observed that as the mixing time was decreased, the nanoparticle size decreased from about 29 to 23 nm for 50 mg/mL polymer concentration and from about 26 to 20 nm for 20 mg/mL polymer concentrations, respectively, which was smaller than the 30−35 nm size obtained by bulk nanoprecipitation. Furthermore, nanoparticle size distributions obtained using dynamic light scattering indicated an increase in the homogeneity of the nanoparticles as the rate of mixing was increased (Figure 3).

Self-assembly of the diblock copolymers during nanoprecipitation is currently believed to occur in three stages (Figure 1a).[26] In the first stage, nuclei consisting of several unimers are formed when the diblock polymer experiences a change in the solvent. In the second stage, these nuclei grow in size through a diffusion-limited process by addition of more unimers. This process continues until the nanoparticles grow sufficiently large and addition of more unimers becomes difficult due to the formation of a polymer brush layer on the nanoparticle surface. The end of the second stage results in kinetically locked nanoparticles. The third stage is characterized by extremely slow changes in the nanoparticle size due to exchange of unimers in order to reach equilibrium. Often, the nanoparticles may degrade before equilibrium is reached. If mixing is not complete during aggregation of the unimers, the barrier to aggregation and addition of unimers

is lowered, leading to the formation of larger nanoparticles. However, if mixing occurs faster than the time scale for aggregation of the nanoparticles, i.e., $\tau_{mix} < \tau_{agg}$, the nanoparticle size may be expected to become independent of mixing time and polymer concentration. The result is kinetically locked nanoparticles that are smaller in size and are expected to be more homogeneous than the particles prepared by slow mixing.[26] By use of an impinging jet mixer, this time scale was found to be in the range of 26−60 ms for polybutylacrylate-*b*-poly(acrylic acid) (PBA(59)-PAA(104)) copolymers for concentrations ranging from 0.1 to 0.65% w/w.[26]

While the observed decrease in nanoparticle size and increase in homogeneity with a decrease in mixing time were consistent with this model of self-assembly of diblock copolymers during nanoprecipitation,[26,27] the PLGA-PEG nanoparticles showed an unexpected consistent decrease in size as the relative flow rate of the polymer stream was decreased. This phenomenon implies that either the polymer concentration or mixing time (or both) affects nanoparticle size even at relatively rapid rates of mixing. One possibility is that there is a time scale associated with rearrangement of the diblock polymers during the growth nanoparticles, i.e., the small PEG block requires time to make its way to the surface of the nascent nanoparticle. As a result, slower self-assembly by decrease of polymer concentration or polymer flow rate may result in the formation of smaller nanoparticles. However, further investigation is required to verify this hypothesis.

Effect of Polymer Composition on Nanoparticle Size. We also examined the effect of polymer composition on nanoprecipitation by adding different amounts of PLGA polymer to the PLGA-PEG diblock polymer. We hypothesized that addition of PLGA to PLGA-PEG nanoparticles may enable control of nanoparticle composition and properties, which may be used to control drug encapsulation and release. However, nanoprecipitation of mixtures of PLGA and PLGA-PEG by bulk synthesis results in large nanoparticles,[12–14] and we were interested in exploring whether rapid mixing improved this size distribution. Precursor composition was varied by addition of $PLGA_{100K}$ to $PLGA_{15K}$-$PEG_{3.4K}$, and the sizes of nanoparticles formed by nanoprecipitation in bulk and by hydrodynamic flow focusing were compared. Addition of PLGA had a large effect on bulk nanoprecipitation, and the *Z*-average nanoparticle diameter increased from 30 to 105 nm as the PLGA content was increased to 20% w/w (Figure 4a). Dynamic light scattering revealed a bimodal distribution of large nanoparticles with a broad size distribution (50−300 nm) in addition to the 30 nm nanoparticles. In contrast, the nanoparticle size increased from 24 nm to only 34 nm for on-chip nanoprecipitation for the same increase in PLGA content. Interestingly, size distribution by dynamic light scattering showed a unimodal nanoparticle size distribution with absence of larger aggregates for nanoparticles prepared by hydrodynamic flow focusing. These observations indicate that addition of PLGA decreased the barrier to nanoparticle/polymer aggregation and favored the formation of larger nanoparticles under conditions of slow mixing. However, rapid mixing by hydrodynamic flow

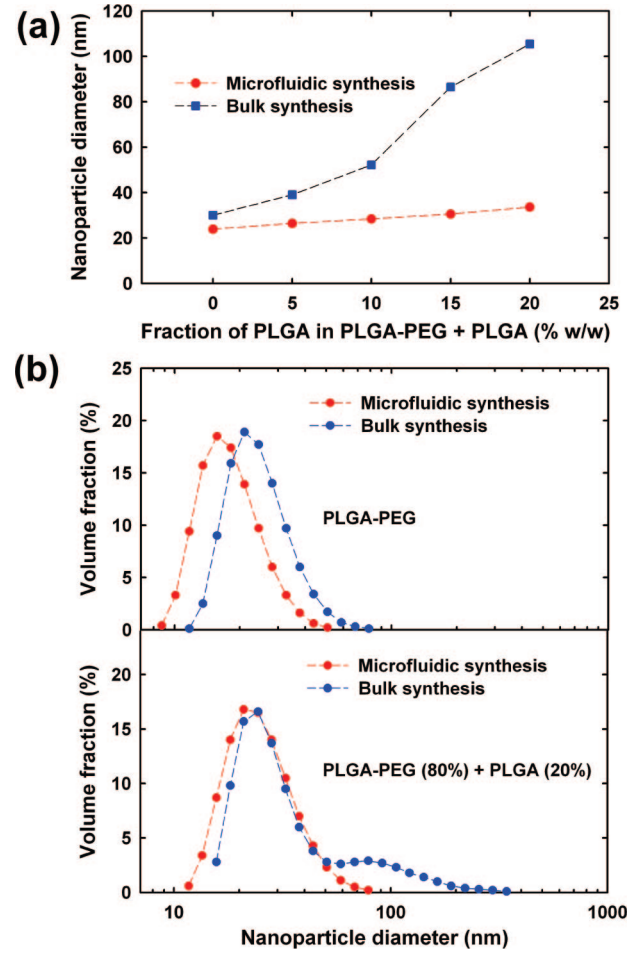

Figure 4. Effect of polymer composition on nanoprecipitation. (a) Size of nanoparticles prepared by bulk nanoprecipitation of $PLGA_{15K}$-$PEG_{3.4K}$ increased dramatically as increasing amounts of free $PLGA_{100K}$ were added to the precursor solution. However, the size of nanoparticles prepared by hydrodynamic flow focusing remained relatively unchanged upon addition of $PLGA_{100K}$ (total polymer concentration 50 mg/mL). (b) Comparison of size distributions of nanoparticles in the absence and presence of 20% w/w $PLGA_{100K}$ reveal that $PLGA_{100K}$ induced aggregation of nanoparticles to form a tail of larger nanoparticles under conditions of slow mixing. However, this aggregation did not occur under conditions of rapid mixing in a microfluidic device, preserving the homogeneity and size of the resulting nanoparticles.

focusing prevented nanoparticle aggregation resulting in smaller and more homogeneous nanoparticles. It has been shown that the sensitivity of PLGA-PEG nanoparticle size to precursor concentration increases when the polymer length increases, which may be due to micelle-like structures for smaller PLGA-PEG molecular weights (<30 kDa) and nanosphere-like structures at higher molecular weights.[24] Our results are consistent with this and indicate that polymer composition plays a significant role in determining the sensitivity of nanoprecipitation to the rate of mixing.

Effect of Polymer Composition and Mixing Time on Drug Loading and Release. We next investigated the use of microfluidic mixing to assemble drug-encapsulated nanoparticles. Using docetaxel (Dtxl) as a model therapeutic agent, we postulated that Dtxl loading may be maximized

and Dtxl release rate may be prolonged by adding hydrophobic PLGA to the PLGA-PEG nanoparticle. As demonstrated in Figure 4a, bulk precipitation of PLGA-PEG with additional PLGA results in larger nanoparticles; the presence of Dtxl in the nanoprecipitation process may further increase the NP size and polydispersity.[12–14] We therefore explored the possibility of using rapid mixing to tune nanoparticle composition to increase the drug loading, without adversely affecting the size and size distribution. In order to tune the Dtxl loading and encapsulation efficiency, nanoparticles prepared using a mixture of 80% $PLGA_{15K}$-$PEG_{3.4K}$ and 20% $PLGA_{100K}$ were compared with nanoparticles synthesized using only $PLGA_{15K}$-$PEG_{3.4K}$. The precursor solution was 25 mg/mL polymer (nominally either 100% PLGA-PEG or 80% PLGA-PEG and 20% PLGA) and 5 mg/mL Dtxl in acetonitrile. Nanoparticles were synthesized using flow focusing at flow rates of 100 and 5 μL/min for the water and acetonitrile streams, respectively. The higher flow rate was essential for higher throughput required for the drug release study. With Dtxl in the acetonitrile stream, we observed some precipitation in the microchannel, but it did not significantly change the flow characteristics. For comparison, nanoparticles were prepared in bulk by pipetting the same acetonitrile solution into water. Care was taken to centrifuge and wash the nanoparticles with sufficient quantity of water to ensure that there was no residual free drug during subsequent analysis (see Supporting Information).

Dtxl loading is defined as the mass fraction of drug Dtxl in the nanoparticles, whereas encapsulation efficiency is the fraction of initial Dtxl that is encapsulated by the nanoparticles. As shown in Figure 5, the Dtxl encapsulation efficiency and mass loading nearly doubled upon increasing the content of free PLGA in the precursor solution. With addition of PLGA, the encapsulation efficiency increased from 28% to 51% and the drug loading increased from 4.1% to 6.8% in the case of microfluidic synthesis. For bulk synthesis, encapsulation efficiency increased from 21% to 45% and drug loading increased from 3.1% to 6.0%. This observation shows that increasing the PLGA content of nanoparticles can increase their hydrophobicity and thus increase the drug encapsulation.

Addition of PLGA also decreased the Dtxl release rates in the case of both bulk and microfluidic synthesis. Drug release (defined as the mass fraction of total drug released, see Supporting Information) was relatively rapid with a similar half-life of approximately 5−6 h in the case of nanoparticles prepared by bulk and microfluidic synthesis without addition of PLGA. Upon addition of $PLGA_{100K}$, the release rate decreased significantly, resulting in the half-life increasing to approximately 11 h in the case of bulk nanoprecipitation. However, this increase in half-life was higher in the case of nanoprecipitation by flow focusing, which resulted in a half-life of approximately 19 h.

Consistent with addition of PLGA to PLGA-PEG without drug (Figure 4), the nanoparticle size increased considerably upon addition of $PLGA_{100K}$ to the precursor solution (Figure 6). Nanoparticles produced by flow focusing were smaller in size than those produced in bulk, and this difference was

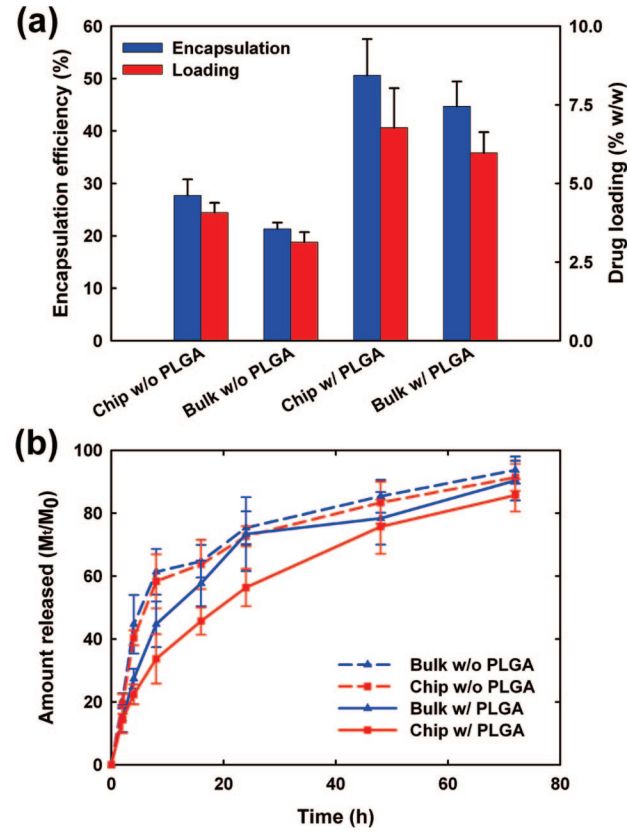

Figure 5. Drug loading and release of PLGA-PEG nanoparticles with Dtxl. (a) Encapsulation efficiency and drug loading of nanoparticles obtained by hydrodynamic flow focusing and bulk nanoprecipitation of 25 mg/mL polymer ($PLGA_{15K}$-$PEG_{3.4K}$ (w/o PLGA)and 80% $PLGA_{15K}$-$PEG_{3.4K}$ with 20% $PLGA_{100K}$ w/w (w/ PLGA)) and 5 mg/mL Dtxl revealed that drug loading and encapsulation nearly doubled upon addition of PLGA, with nanoprecipitation on chip resulting in a slightly higher encapsulation and loading. (b) Drug release rates were highest for nanoparticles prepared without addition of $PLGA_{100K}$ and did not differ significantly between bulk and chip synthesis. Addition of $PLGA_{100K}$ to the precursor solution dramatically decreased the release rates, but the effect was significantly larger in the case of nanoparticles prepared on chip, which showed the slowest drug release. Error bars denote 95% confidence ($n = 3$).

markedly more evident when $PLGA_{100K}$ was added to the precursors. Thus, the nanoparticle size dependence on rate of mixing remained qualitatively the same upon addition of Dtxl to the precursor solution. However, there was an overall increase in size of nanoparticles upon addition of Dtxl. In order to probe the surface charge of the nanoparticles, we measured the zeta potential. The zeta potential values of the nanoparticles were negative, which is expected because the PEG terminals have a negatively charged carboxyl end. Interestingly, the zeta potential of nanoparticles prepared by flow focusing remained nearly unchanged at −28 mV upon addition of PLGA to the precursors. However, the zeta potential decreased from −27 to −19 mV upon addition of PLGA to the precursors in the case of bulk nanoprecipitation (Figure 6). We observed the same trend in zeta potential in the absence of Dtxl, where the zeta potential of nanoparticles prepared by rapid mixing remained essentially unchanged upon addition of PLGA (−29 mV), while the zeta potential

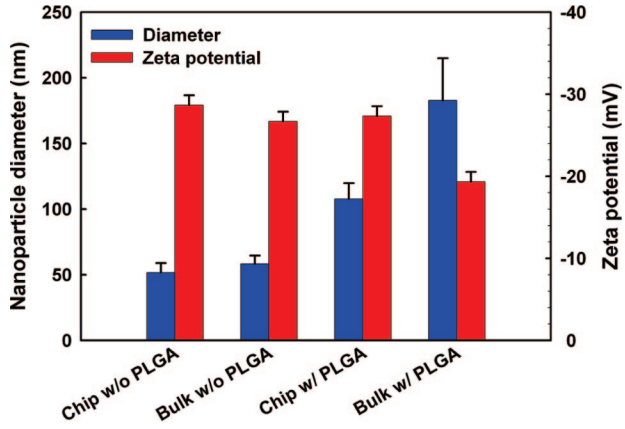

Figure 6. Size and zeta potential of PLGA-PEG nanoparticles with Dtxl. Nanoparticles obtained by hydrodynamic flow focusing and bulk nanoprecipitation of 25 mg/mL polymer ($PLGA_{15K}$-$PEG_{3.4K}$ (w/o PLGA)and 80% $PLGA_{15K}$-$PEG_{3.4K}$ with 20% $PLGA_{100K}$ w/w (w/ PLGA)) and 5 mg/mL Dtxl showed an increase in *Z*-average size upon addition of $PLGA_{100K}$. The increase in size was less striking for nanoparticles prepared by hydrodynamic flow focusing as compared to bulk nanoprecipitation. The zeta potential did not change significantly upon addition of $PLGA_{100K}$ in the case of nanoprecipitation on chip, but the zeta potential decreased significantly in magnitude in the case of bulk nanoprecipitation. Error bars denote 95% confidence ($n = 3$).

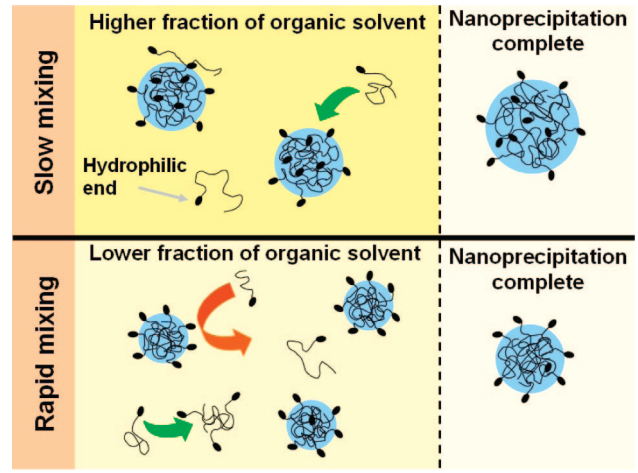

Figure 7. Mechanism of self-assembly of nanoparticles during nanoprecipitation. Slow mixing ($\tau_{mix} > \tau_{agg}$) results in aggregation of polymers to form nanoparticles when mixing is incomplete, and thus occurs in the presence of higher fraction of organic solvent in the solution. Under these conditions, polymers easily adsorb on nanoparticle aggregates, burying hydrophilic end groups and leading to formation of larger nanoparticles. Rapid mixing ($\tau_{mix} < \tau_{agg}$) results in aggregation of polymers when mixing is nearly complete, and thus occurs in the presence of a lower fraction of organic solvent in the solution. Polymers cannot easily adsorb or insert into nanoparticles and nucleate more nanoparticles that are smaller in size with fewer hydrophilic end groups buried inside the nanoparticle.

of nanoparticles prepared by bulk mixing decreased from −27 to −20 mV.

Mechanism of Self-Assembly. These observations give some insights into the role of solvent/nonsolvent mixing in self-assembly of nanoparticles during nanoprecipitation. It has been shown that the rate of drug release and the zeta potential are affected by nanoparticle composition, size, and drug loading.[24] Previous studies have also demonstrated that PEG terminals are incorporated in the interior of PLGA-PEG nanoparticles prepared by nanoprecipitation, especially when the length of the PLGA block is large compared to the length of the PEG block.[28] Incorporation of PEG in the nanoparticle may be expected to increase the rate of drug release by facilitating diffusion though loosely packed hydrophilic water and PEG pockets in the nanoparticle. Concomitantly, as a larger fraction of charged PEG and PLGA terminals get incorporated into the nanoparticle, the net surface charge on the nanoparticle is expected to decrease as more carboxyl terminals are buried inside the nanoparticle, leading to a decrease in the zeta potential. Indeed, these trends of decreased zeta potential and increased rate of drug release despite larger nanoparticle size were observed in the case of nanoparticles prepared by bulk nanoprecipitation when $PLGA_{100K}$ was added to the precursor solution. This suggests that nanoprecipitation through slower mixing results in a higher proportion of PEG incorporation in the nanoparticles during self-assembly in addition to increased particle size. This is reasonable if we consider the process of nanoprecipitation under rapid and slow mixing (Figure 7). Under rapid microfluidic mixing, solvent exchange is complete even before the polymers begin aggregating. Therefore, nanoparticle assembly occurs in solvent conditions that more closely match the final solvent, i.e., water with a small fraction (5%) of acetonitrile. However, under bulk mixing, the time scale of nanoparticle assembly is smaller than the time scale of solvent exchange. Thus, nanoparticle assembly occurs in solvent conditions that are very different from the final solvent condition; i.e., assembly occurs when the fraction of acetonitrile in the solution is larger than that in the final solvent. Previous studies have suggested a mechanism in which the barrier to insertion of polymers from the solution into nanoparticles is lower when solvent exchange is incomplete, leading to an increased nanoparticle size. However, we observed that the polymers formed large aggregates of sizes up to 1 μm in water−acetonitrile mixtures with a significant fraction of acetonitrile, which is not possible unless hydrophilic polymer terminals are buried inside the nanoparticle (see Supporting Information). This indicates that in addition to increasing the barrier for insertion of polymers into the nanoparticle, incomplete mixing during nanoprecipitation facilitates adsorption of the polymers on existing polymers, thereby burying hydrophilic ends inside the nanoparticle. This effect is magnified when $PLGA_{100K}$ is added to the precursor solution, which is consistent with the increased sensitivity to copolymer concentration and solvent conditions observed for higher molecular weight (>45 kDa) PLGA-PEG.[24,28] Similar effects may result in larger nanoparticles when the ratio of organic solvent to water is increased during nanoprecipitation.[24]

We also investigated the water/acetonitrile ratio at which each precursor starts precipitating by gradually adding water to a solution of each precursor in acetonitrile. We observed precipitation of PLGA and PLGA-PEG around a water content of 25% v/v, while that of Dtxl occurred at a higher water content of about 45% v/v. It indicates that Dtxl starts precipitating after the polymer, and rapid mixing may

actually yield slightly lower drug encapsulation as some drug may be "locked out" of the nanoparticles that have already formed before the drug starts precipitating. However, this effect may be offset by rapid solvent exchange in microfluidic synthesis as the solubility of the drug in a solvent with a higher fraction of water is lower than that in a solvent with a higher fraction of acetonitrile, which is the case of bulk synthesis. These differing time scales of solvent exchange and self-assembly offer interesting possibilities for improving nanoparticle characteristics. Control of reactions over time is easily possible using microfluidic devices[6] and offers unique methods of engineering multistep nanoprecipitation processes for optimization of drug loading in these nanoparticles. Use of microfluidics to understand and control nanoprecipitation offers exciting avenues in the future for tailoring the properties of nanoparticles through controlled self-assembly.

Conclusion. Herein we demonstrate that microfluidics is a useful technology for nanoprecipitation synthesis of smaller and more homogeneous PLGA-PEG nanoparticles as compared to bulk synthesis. Microfluidics enables control over the rate of mixing, and in conjunction with controlling precursor composition, it may be used to tune nanoparticle size, homogeneity, and drug loading and release. Our work suggests that microfluidic synthesis of nanoparticles by self-assembly of polymeric precursors may enable better control over the physicochemical properties of nanoparticles and may prove to be useful in the emerging field of nanomedicine.

Acknowledgment. We thank MIT's Microsystems Technology Laboratory and staff for their help with device fabrication. We also thank Sangeeta Bhatia (MIT) for graciously allowing the use of particle sizing equipment in her laboratory. Negative staining sample preparation and electron microscopy image acquisition were performed by Eliza Vasile, from the Center for Cancer Research, Microscopy and Imaging Core Facility, MIT. This research was supported by the Koch-Prostate Cancer Foundation Award in Nanotherapeutics (R.L. and O.C.F.), by a Concept Development Grant from the Dana Farber Cancer Institute Prostate SPORE (O.C.F.), and by NIH Grants CA119349 (R.L. and O.C.F.) and EB003647 (O.C.F.). F.G. was supported by a Postdoctoral Fellowship from the Canadian Natural Sciences and Engineering Research Council.

Note Added after ASAP Publication: There was a change to the Acknowledgment in the version published ASAP July 26, 2008; the corrected version was published ASAP July 30, 2008.

Supporting Information Available: A description of experimental methods. This material is available free of charge via the Internet at http://pubs.acs.org.

References

(1) DeMello, J.; DeMello, A. *Lab Chip* **2004**, *4* (2), 11N–15N.
(2) deMello, A. J. *Nature* **2006**, *442* (7101), 394–402.
(3) Yen, B. K. H.; Stott, N. E.; Jensen, K. F.; Bawendi, M. G. *Adv. Mater.* **2003**, *15* (21), 1858–1862.
(4) Nguyen, N. T.; Wu, Z. G. *J. Micromech. Microeng.* **2005**, *15* (2), R1–R16.
(5) Wagner, J.; Kohler, J. M. *Nano Lett.* **2005**, *5* (4), 685–691.
(6) Shestopalov, I.; Tice, J. D.; Ismagilov, R. F. *Lab Chip* **2004**, *4* (4), 316–321.
(7) Krishnadasan, S.; Brown, R. J.; deMello, A. J.; deMello, J. C. *Lab Chip* **2007**, *7* (11), 1434–1441.
(8) De Mello, A., De Mello, J., Edel, J. *Preparation of nanoparticles*. U.S. Patent 7,252,814, 2006.
(9) Chan, E. M.; Alivisatos, A. P.; Mathies, R. A. *J. Am. Chem. Soc.* **2005**, *127* (40), 13854–13861.
(10) Xu, S.; Nie, Z.; Seo, M.; Lewis, P.; Kumacheva, E.; Stone, H. A.; Garstecki, P.; Weibel, D. B.; Gitlin, I.; Whitesides, G. M. *Angew. Chem., Int. Ed.* **2005**, *44* (5), 724–728.
(11) Quintanar-Guerrero, D.; Allemann, E.; Fessi, H.; Doelker, E. *Drug Dev. Ind. Pharm.* **1998**, *24* (12), 1113–1128.
(12) Zhang, H.; Tumarkin, E.; Sullan, R. M. A.; Walker, G. C.; Kumacheva, E. *Macromol. Rapid Commun.* **2007**, *28* (5), 527–538.
(13) Gref, R.; Minamitake, Y.; Peracchia, M. T.; Trubetskoy, V.; Torchilin, V.; Langer, R. *Science* **1994**, *263* (5153), 1600–1603.
(14) Farokhzad, O. C.; Cheng, J. J.; Teply, B. A.; Sherifi, I.; Jon, S.; Kantoff, P. W.; Richie, J. P.; Langer, R. *Proc. Natl. Acad. Sci. U.S.A.* **2006**, *103* (16), 6315–6320.
(15) Davaran, S.; Rashidi, M. R.; Pourabbas, B.; Dadashzadeh, M.; Haghshenas, N. M. *Int. J. Nanomed.* **2006**, *1* (4), 535–539.
(16) Cheng, J.; Teply, B. A.; Sherifi, I.; Sung, J.; Luther, G.; Gu, F. X.; Levy-Nissenbaum, E.; Radovic-Moreno, A. F.; Langer, R.; Farokhzad, O. C. *Biomaterials* **2007**, *28* (5), 869–876.
(17) Xu, S.; Nie, Z.; Seo, M.; Lewis, P.; Kumacheva, E.; Stone, H. A.; Garstecki, P.; Weibel, D. B.; Gitlin, I.; Whitesides, G. M. *Angew. Chem., Int. Ed.* **2005**, *44* (25), 3799–3799.
(18) Seo, M.; Nie, Z. H.; Xu, S. Q.; Mok, M.; Lewis, P. C.; Graham, R.; Kumacheva, E. *Langmuir* **2005**, *21* (25), 11614–11622.
(19) Martin-Banderas, L.; Flores-Mosquera, M.; Riesco-Chueca, P.; Rodriguez-Gil, A.; Cebolla, A.; Chavez, S.; Ganan-Calvo, A. M. *Small* **2005**, *1* (7), 688–692.
(20) Nisisako, T.; Torii, T.; Higuchi, T. *Chem. Eng. J.* **2004**, *101* (1−3), 23–29.
(21) De Geest, B. G.; Urbanski, J. P.; Thorsen, T.; Demeester, J.; De Smedt, S. C. *Langmuir* **2005**, *21* (23), 10275–10279.
(22) Anna, S. L.; Bontoux, N.; Stone, H. A. *Appl. Phys. Lett.* **2003**, *82* (3), 364–366.
(23) Owens, D. E.; Peppas, N. A. *Int. J. Pharm.* **2006**, *307* (1), 93–102.
(24) Avgoustakis, K. *Curr. Drug Delivery* **2004**, *1* (4), 321–333.
(25) Knight, J. B.; Vishwanath, A.; Brody, J. P.; Austin, R. H. *Phys. Rev. Lett.* **1998**, *80* (17), 3863–3866.
(26) Johnson, B. K.; Prud'homme, R. K. *Phys. Rev. Lett.* **2003**, *91* (11), 118302.
(27) Matteucci, M. E.; Hotze, M. A.; Johnston, K. P.; Williams, R. O. *Langmuir* **2006**, *22* (21), 8951–8959.
(28) Riley, T.; Stolnik, S.; Heald, C. R.; Xiong, C. D.; Garnett, M. C.; Illum, L.; Davis, S. S.; Purkiss, S. C.; Barlow, R. J.; Gellert, P. R. *Langmuir* **2001**, *17* (11), 3168–3174.

NL801736Q